The Immp2l Mutation Causes Ovarian Aging Through ROS-Wnt/β-Catenin-Estrogen Pathway: Preventive Effect of Melatonin

Qing He,[1*] Lifang Gu,[1*] Qingyin Lin,[1*] Yi Ma,[1] Chunlian Liu,[1] Xiuying Pei,[1] P. Andy Li,[2] and Yanzhou Yang[1]

[1]Key Laboratory of Fertility Preservation and Maintenance, Ministry of Education, Key Laboratory of Reproduction and Genetics in Ningxia, Department of Histology and Embryology, Department of Pathology, Ningxia Key Laboratory of Cerebrocranial Diseases, Incubation Base of National Key Laboratory, Department of Center for Reproductive Medicine, General Hospital, Ningxia Medical University, Yinchuan, Ningxia 750001, P.R. China; and [2]Department of Pharmaceutical Sciences, Biomanufacturing Research Institute and Technological Enterprise (BRITE), College of Health and Sciences, North Carolina Central University, Durham, North Carolina 27707

ORCiD number: 0000-0002-1220-5164 (Y. Yang).

Mitochondria play important roles in ovarian follicle development. Mitochondrial dysfunction, including mitochondrial gene deficiency, impairs ovarian development. Here, we explored the role and mechanism of mitochondrial inner membrane gene *Immp2l* in ovarian follicle growth and development. Our results revealed that female Immp2l$^{-/-}$ mice were infertile, whereas Immp2l$^{+/-}$ mice were normal. Body and ovarian weights were reduced in the female Immp2l$^{-/-}$ mice, ovarian follicle growth and development were stunted in the secondary follicle stage. Although a few ovarian follicles were ovulated, the oocytes were not fertilized because of mitochondrial dysfunction. Increased oxidative stress, decreased estrogen levels, and altered genes expression of Wnt/β-catenin and steroid hormone synthesis pathways were observed in 28-day-old Immp2l$^{-/-}$ mice. The Immp2l mutation accelerated ovarian aging process, as no ovarian follicles were detected by age 5 months in Immp2l$^{-/-}$ mice. All the aforementioned changes in the Immp2l$^{-/-}$ mice were reversed by administration of antioxidant melatonin to the Immp2l$^{-/-}$ mice. Furthermore, our in vitro study using Immp2l knockdown granulosa cells confirmed that the Immp2l downregulation induced granulosa cell aging by enhancing reactive oxygen species (ROS) levels, suppressing *Wnt16*, increasing β-catenin, and decreasing steroid hormone synthesis gene *cyp19a1* and estrogen levels, accompanied by an increase in the aging phenotype of granulosa cells. Melatonin treatment delayed granulosa cell aging progression. Taken together, Immp2l causes ovarian aging through the ROS-Wnt/β-catenin-estrogen (cyp19a1) pathway, which can be reversed by melatonin treatment. **(*Endocrinology* 161: 1–17, 2020)**

Key Words: ovarian aging, Immp2l Mutation, ROS, Wnt/β-catenin, estrogen, granulosa cells, mitochondrion

Female fertility is primarily determined by the ovarian lifespan. Decreased fertility or infertility is caused by the shortening of the ovarian lifespan, which is attributed to ovarian aging (1). The phenotype of ovarian aging includes an increase in fibrous tissue, a decrease in the number of primordial follicle, a reduction in oocyte quality, diminishment of follicles and oocytes, and a decline in the antral follicular count (2, 3).

ISSN Online 1945-7170

Received 10 May 2020. Accepted 9 July 2020.
First Published Online 11 July 2020.
Corrected and Typeset 21 August 2020.

*Q.H., L.G., and Q.L. contributed equally to this work.

Abbreviations: AMH, anti-Müllerian hormone; co-IP, coimmunoprecipitation; E2, estrogen; FZ, frizzle; GSH-Px, glutathione peroxidase; Immp2l, inner mitochondrial membrane peptidase 2-like; MDA, malondialdehyde; OS, oxidative stress; ROS, reactive oxygen species; siRNA, small interfering RNA.

Mitochondria are the most prominent organelles in the oocyte. Oocyte mitochondria inherited by offspring and mitochondrial from the sperm are degraded immediately after fertilization (4). The mitochondrial genome also plays a vital role in ovarian follicle development (5). Mitochondrial dysfunction triggers ovarian dysfunction, infertility, and ovarian aging (6). Mitochondria are the primary source of intracellular reactive oxygen species (ROS), and mitochondrial dysfunction increases ROS production. Physiological levels of ROS are essential for normal ovarian function. However, excessive ROS may overpower the body's natural antioxidant defense system, causing oxidative stress (OS) damage (7). It has been reported that higher OS in the follicular microenvironment accelerates ovarian aging, whereas long-term OS induced by ozone inhalation reduces ovarian reserve, decreases ovarian function, and results in ovarian aging-related disorders (8).

Inner mitochondrial membrane peptidase 2-like (Immp2l) is a peptidase located on the mitochondrial inner membrane. Mutation of this gene causes elevation of mitochondrial superoxide production without affecting ATP generation or mitochondrial membrane potential (9), augments ischemic brain damage, impairs mitochondrial function (10), results in erectile dysfunction and age-dependent spermatogenesis in male mice and defective oogenesis in female mice (11, 12), reduces food intake (13), and causes bladder dysfunction (14), early onset of ataxia, and kyphosis (15).

Wingless-type mouse mammary tumor virus integration site (Wnt) signaling molecules are locally secreted glycoproteins that play vital roles in several physiological and pathological developmental processes. Wnts are highly conserved signaling molecules that act through β-catenin-dependent (canonical) and β-catenin-independent (noncanonical) pathways. The canonical Wnt signaling is governed by the interaction of β-catenin with other molecules to regulate cellular decisions related to proliferation, differentiation, and morphogenesis (16-18). The vital roles of Wnt/β-catenin pathway, Wnt ligands, and frizzled (FZ) receptor in ovarian follicle growth and development have been highlighted in several studies. These include follicle development, corpus luteum formation, steroid production, and fertility (19). Dysregulation of Wnt/β-catenin pathway, Wnt ligands, and FZ receptor triggers impairment of ovarian follicle development, growth, and even infertility. In particular, previous studies have suggested that Wnt2, Wnt4, and β-catenin regulate the development and growth of ovarian follicle through promoting proliferation of granulosa cells and modulating ovarian β-catenin target genes, Cyp11a1, Cyp19a1, and StAR (20). The important role of Wnt pathway and network in ovarian folliculogenesis has been reviewed by Hernandez (21).

Melatonin is considered as a mitochondrial protector because of its antioxidant capacity. It has been used as a mitochondria-targeted antioxidant to treat aging-related diseases (22, 23). Published result shows that melatonin preserves mitochondrial function and hinders aging and age-associated disorders (24).

The role of the *Immp2l* gene in male and female reproduction has been reported. Immp2l homozygous mutant female mice showed that ovarian follicle development in ovaries of 3-week-old mutant mice did not proceed beyond the preantral/early antral stage, indicating that preantral follicle stage development was normal. However, more preantral follicles and fewer antral follicles were observed in Immp2l$^{-/-}$ mice than in the wild-type mice, as well as degenerating follicles with marked luteinization (12). The accurate role and mechanism of Immp2l in female reproductive system are unknown. Whether Immp2l is involved in ovarian follicle development, whether OS is the primary cause for the losses ovarian follicle in Immp2l mutant mice, and whether ovarian aging can be reversed by treatment with antioxidant melatonin are currently unknown. Therefore, we used Immp2l mutant mice in this study with or without melatonin intervention to delineate the alterations in ovarian follicle development and the underlying molecular pathways.

Methods

Animals

The *Immp2l*$^{Tg(Tyr)979Ove}$ mutant mice were generated according to a previous study, and breeding pairs were received as gifts (12). The mice were bred in an animal facility at Ningxia Medical University and maintained at 24 ± 2°C in a light-controlled room (12-hour light:12-hour darkness) with free access to food and water. Genotyping was performed by PCR using a specific primer, with mouse coat color as a reference. Homozygous normal mice were albino because of the FVB background. Heterozygotes were slightly pigmented because of the expression of tyrosinase from 1 copy of the transgene. Homozygous mutant mice were darkly pigmented from the expression of tyrosinase from 2 copies of the transgene. The animal procedures strictly followed the guidelines from National Institutes of Health and were approved by the Institutional Animal Care and Use Committee at Ningxia Medical University. All animals were operated on under sodium pentobarbital anesthesia and all efforts were made to minimize pain and discomfort.

Histology and ovarian follicle count

Six ovaries of each group were collected, embedded in paraffin, cut into serial sections, and stained using hematoxylin

and eosin. Ovarian follicles were counted according to a previous method (25-27).

RNA sequencing

Total RNA was quantified using a NanoDrop 2000 spectrophotometer (NanoDrop Technologies, Wilmington, DE). The ovaries from 1 side were used for RNA sequencing by Breeding Biotechnologies (China) according to standard procedures, and the ovaries from the other side were used for RT-quantitative PCR. Each group contained at least 3 ovaries.

RT-quantitative PCR

Total RNA extraction and detection were performed according to the methods of our previous studies (25, 26). cDNA was reverse-transcribed using a PrimeScipt RT reagent kit (TaKaRa, Dalian, China), according to the manufacturer's instructions. RT-quantitative PCR was performed using 7500 Software v.2.0.5 (7500 Fast Real-Time PCR System, ABI). The primer sequences and annealing temperatures are provided in Table 1 (Supplemental materials) (28). The mouse *GAPDH* gene, which was used as a reference gene, was amplified in parallel with the target gene, allowing gene expression normalization. Additionally, $2^{-\Delta\Delta}$Ct was used for quantification. The quantitative PCR procedure was conducted using SYBR Premix Ex Taq II (TaKaRa, Dalian, China), according to the manufacturer's instructions.

Western blot analyses

SDS gel electrophoresis was performed according to the methods described in our previous study (25). Briefly, the protein contents of each sample were measured using a BCA kit. Equal amounts of protein samples were loaded onto a 12% SDS gel for electrophoresis. The proteins were transferred onto polyvinylidene difluoride membranes that were blocked for 1 hour with 5% nonfat dry milk and probed with the primary antibodies of anti-Rabbit Immp2l (15970-1-AP, Proteintech) (29), rabbit Cyp19a1 (16554-1-AP, Proteintech) (30), mouse β-catenin (66379-1-Ig, Proteintech) (31), rabbit Wnt16 (ab109437, Abcam) (32), rabbit P21 (ab188224, Abcam) (33), and GAPDH (2118S, Cell Signaling) (34) at 4°C overnight. The membranes were then incubated with an horseradish peroxidase-conjugated anti-rabbit IgG (7074S, Cell Signaling) (35) or anti-mouse IgG (7076S, Cell Signaling) (36) secondary antibody at dilution of 1:2000. The resulting signal was visualized using the ECL Detection Kit (Thermo), according to the manufacturer's instructions. GAPDH was used as loading reference. The relative protein band densities of targeting proteins were measured using Image J Software and presented as a ratio of target protein over the loading control.

Melatonin treatment

The 14-day-old Immp2l homozygous mutant mice were administered with 30 mg/kg (body weight) melatonin once a day at 8:00 AM via IP injection for 2 weeks, according to the methods of a previous study (37, 38). The melatonin-treated mice were then divided into 2 groups; 1 was used to check the morphological changes and related signaling pathways and the other was administered with melatonin-containing water (100 mg/L and 200 mg/L) until 5 months of age (39). For in vitro studies, the granulosa cells were treated with 10 μM melatonin (40).

ROS and oxidative stress

To assess oxidative stress, 1 of the oxidative stress biomarker malondialdehyde (MDA, KGT003-1, KeyGENBioTECH) (41, 42) and antioxidant biomarker glutathione peroxidase (GSH-Px, KGT014, KeyGENBioTECH) (43, 44) were detected in serum and cell medium according to the manufacturer's instructions.

Hormone detection

Estrogen (E_2) and anti-Müllerian hormone (AMH) in the serum and cell medium were detected using a mouse ELISA kit, according to the manufacturer's instructions.

Granulosa cell isolation and transfection

The isolation and culture of granulosa cells were conducted according to the methods of our previous study (25). The granulosa cells were transfected with mouse Immp2l short interfering (siRNA; CACTCCAGACTGGTGAGAAAT) or negative siRNA using Lipo RNAIMAX, according to manufacturer's instructions.

Mitochondrial membrane potential and ATP detection

The ROS levels in granulosa cells were measured using a DHE probe (KGAF019, KeyGENBioTECH), and mitochondrial membrane potential was detected with a TMRM probe (HY-D0984, MedChemExpress), according to the manufacturer's protocols. ATP content was measured using an ATP Bioluminescence Assay Kit (Beyotime Institute of Biotechnology), according to the manufacturer's protocols.

Cell cycle

The cell cycle was determined using propidium iodide (Sigma) staining coupled with flow cytometry.

Cell apoptosis

Annexin V/propidium iodide staining was used to detect apoptotic cells. Three days after transfection, 5×10^5 cells were collected and washed twice with ice-cold PBS. The cells were then stained using Alexa Fluor 488 annexin V and propidium iodide (Alexa Fluor 488 annexin V/Dead Cell Apoptosis Kit) and detected using flow cytometry (BestBio), according to the manufacturer's guidelines. Untreated cells served as a negative control.

Cell senescence

Detection of the senescence of granulosa cells was achieved with β-Galactosidase (Gal, KGPAG001, China) and the process was conducted according to the manufacturer's guidelines.

Immunofluorescence

Immunofluorescent staining of target proteins was performed according to our previous protocol (25).

Coimmunoprecipitation

Granulosa cells from the control, Immp2l knockdown, and melatonin treated Immp2l knockdown groups were collected and washed with PBS. The cells were then lysed with RIPA cell lysis buffer. The protein was incubated with 4 μL anti-β-catenin antibody (31) overnight, then incubated with Protein A/G Magnetic Beads (Thermo Scientific) for 2 hours with rotation, and finally washed with lysis buffer. The beads were then placed in 20 μL of 3X Reducing SDS Loading Buffer and heated at 95°C for 5 minutes. The protein effluent was collected using a Magnetic Separation Rack for immunoprecipitation and the supernatant was used for β-catenin detection of output. The granulosa cell proteins from the control, Immp2l knockdown, and melatonin-treated Immp2l knockdown groups were used as input. Then, the magnetic separated protein was loaded directly onto a 12% polyacrylamide gel, as previously described for immunoblotting (26).

Statistical analyses

For the animal study, each group consisted of at least 6 animals. For the in vitro study, all experiments were repeated at least 3 times with a triplicate each time. The data are presented as mean ± SEM. Data were analyzed with ANOVA followed by Fisher's least significant difference test using SPSS software (version 13.0; SPSS, Inc., Chicago, IL). The body and ovarian weights between wild-type and homozygous mutant mice were analyzed with a *t* test using GraphPad Prism. Differences were considered significant at $P < 0.05$.

Results

Homozygous mutant Immp2l caused infertility and delayed ovarian follicle development in female mice

Six- to 8-week-old female wild ($Immp2l^{+/+}$), heterozygous mutation ($Immp2l^{+/-}$), and homozygote mutation ($Immp2l^{-/-}$) mice were mated with 6- to 8-week-old proven fertile wild and heterozygous male mice, respectively. Homozygote mutant male mice were infertile because of erectile dysfunction (12). Fertility was not affected in female heterozygous mutant mice; however, the female homozygote mutant mice were infertile (Fig. 1A and 1B). Furthermore, both the body and ovarian weights were remarkably decreased in the homozygous mutant mice, compared with the wild-type mice at the age of 21 (Fig. 1C and 1E) and 28 (Fig. 1D and 1F) days.

To assess whether the infertility of $Immp2l^{-/-}$ female mice was associated with ovarian follicle growth and development, we examined ovarian morphology in the mutant and wild-type mice using hematoxylin and eosin staining at the ages of 14, 21, and 28 days. The results demonstrated that the ovarian follicle development and growth of 14-day-old $Immp2l^{-/-}$ mice (Fig. 2b and 2B) were normal compared with those of wildtype mice (Fig. 2a and 2A). But the growth of ovarian follicles was delayed at secondary follicle stages in $Immp2l^{-/-}$ mice at 21 days (Fig. 2d and 2D), compared with control mice (Fig. 2c and 2C). This phenotype was confirmed in the $Immp2l^{-/-}$ mice at 28 days (Fig. 2f and 2F). Therefore, there were fewer antral follicles detected in

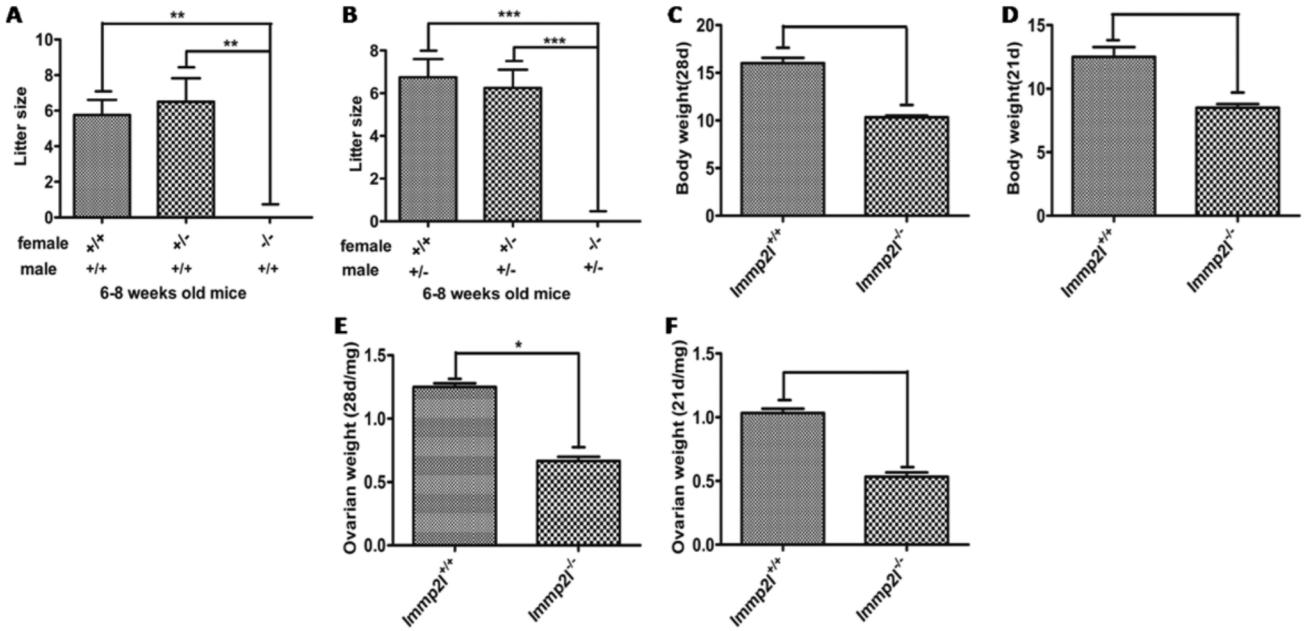

Figure 1. Fertility, body weight, and ovarian weight in $Immp2l^{+/+}$ and $Immp2l^{-/-}$ mice. (A,B) Female $Immp2l^{-/-}$ mice were infertile; (C,D) body weights of $Immp2l^{-/-}$ mice were decreased in 21 and 28 days; (E,F) ovarian weights of $Immp2l^{-/-}$ decreased in 21 and 28 days. Immp2l, inner mitochondrial membrane peptidase 2-like. $^{*}P < 0.05$, $^{**}P < 0.01$, $^{***}P < 0.001$.

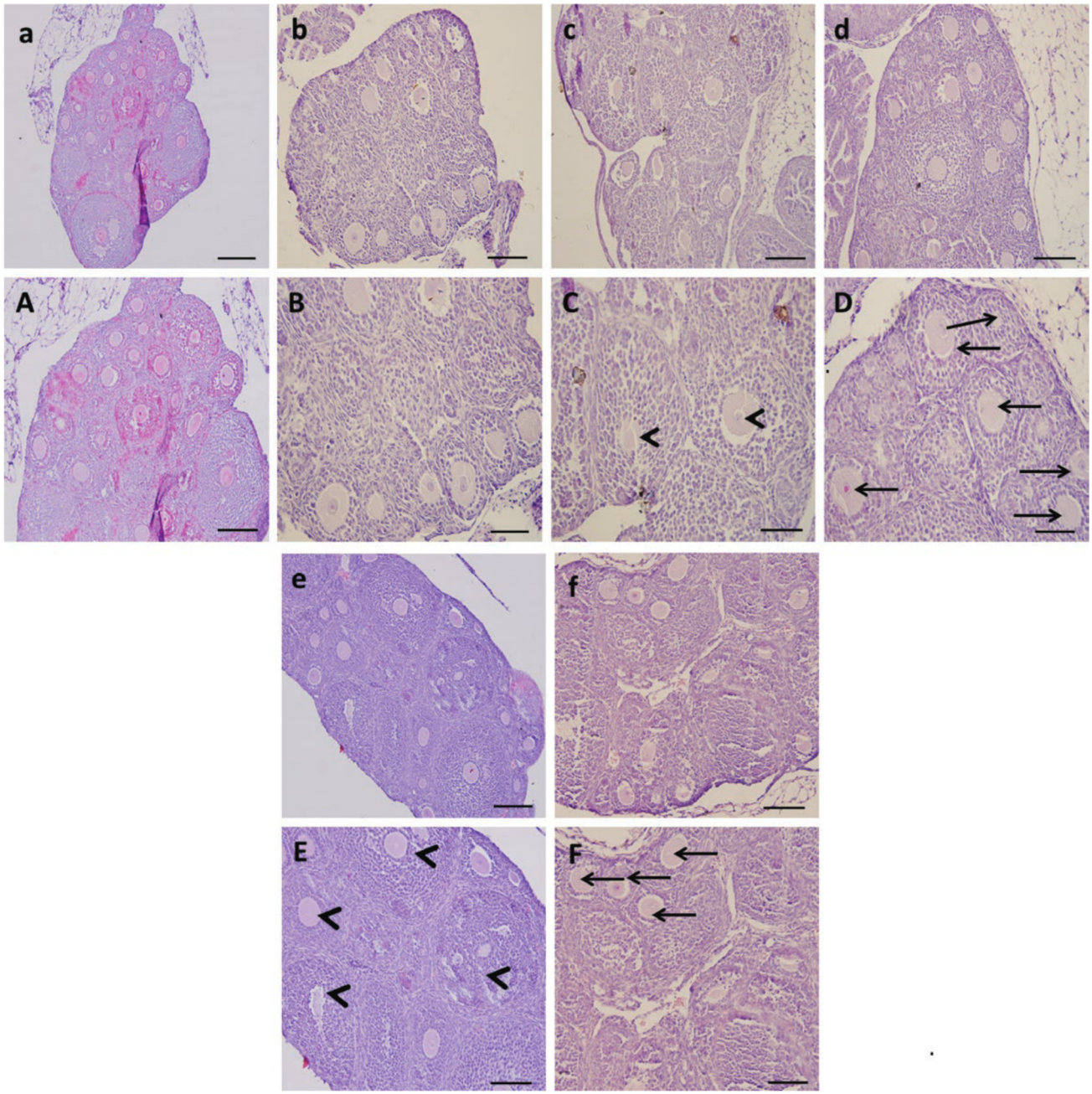

Figure 2. Histological sections showing ovarian morphology in 14-, 21-, and 28-day-old Immp2l$^{-/-}$ mutation mice. (a, A)14-day-old Immp2l$^{+/+}$ mice; (b, B)14-day-old Immp2l$^{-/-}$ mice; (c, C) 21-day-old Immp2l$^{+/+}$ mice; (d, D) 21-day-old Immp2l$^{-/-}$ mice; (e ,E) 28-day-old Immp2l$^{+/+}$ mice; (f, F) 28-day-old Immp2l$^{-/-}$ mice. Growth of ovarian follicles was delayed at secondary follicle stages in Immp2l$^{-/-}$ mice at 21 and 28 days. Arrowheads: antral follicle; arrows: secondary follicle. Scale bar in a-f = 100 μm and in A-F = 50 μm. Immp2l, inner mitochondrial membrane peptidase 2-like.

the Immp2l$^{-/-}$ mice than in the control mice at 28 days (Fig. 2e and 2E). This phenotype was further confirmed by the results from the 35-day-old Immp2l$^{-/-}$ mice (Supplemental Fig. 1) (28).

Immp2l knockout altered the Wnt/β-catenin and estrogen pathways in the ovarian tissue

Based on the morphological observation of ovaries, we counted the number of ovarian follicle and found the number of primordial follicles reduced in 21-day-old Immp2l$^{-/-}$ mice compared with control mice; however, this difference did not reach statistical significance (Fig. 3). The number of primordial follicles was significantly decreased in 28- and 35-day-old mice compared with wild-type mice ($P < 0.05$). Similarly, the number of primary follicles was not altered in 21-day-old Immp2l$^{-/-}$ mice, nonsignificantly decreased in 28-day-old mice, and significantly declined in 35-day-old mice compared with wild-type mice ($P < 0.05$). Moreover, the number of secondary follicles was significantly increased in Immp2l$^{-/-}$ mice at 21, 28, and 35 days compared with the wild-type mice ($P < 0.05$). The increased number of secondary

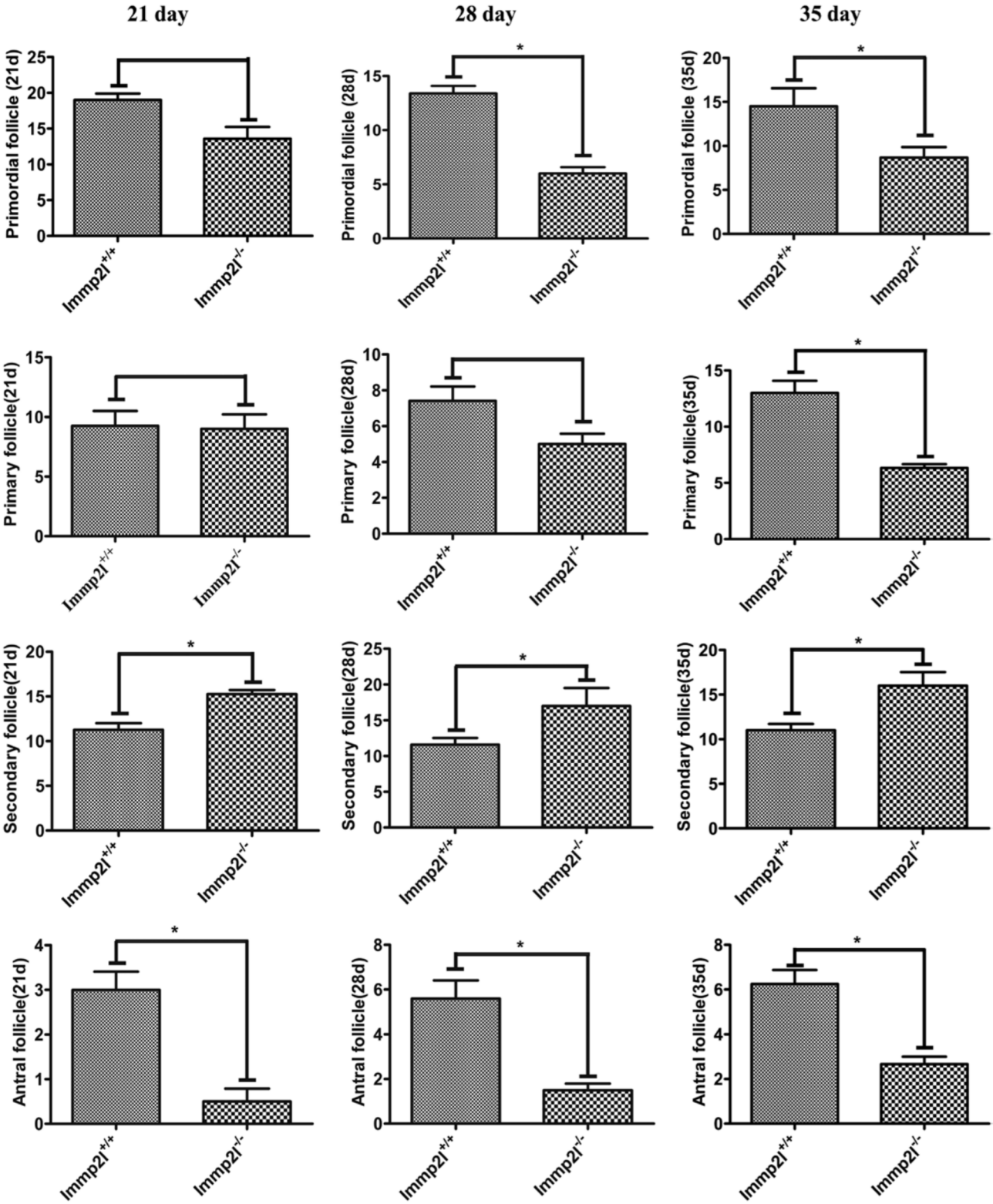

Figure 3. Numbers of primordial, primary, secondary, and antral follicles in the ovaries of 21-, 28-, and 35-day-old Immp2l$^{+/+}$ and Immp2l$^{-/-}$ mice. Homozygous mutation of Immp2l reduced the numbers of primordial, primary, and antral follicles and increased numbers of secondary follicles. Immp2l, inner mitochondrial membrane peptidase 2-like. *$P < 0.05$, **$P < 0.01$, ***$P < 0.001$.

follicles might be due to retarded development of ovarian follicle. Finally, the number of antral follicles was significantly reduced in Immp2l$^{-/-}$ mice at 21, 28, and 35 days compared with the wild-type mice ($P < 0.05$).

To explore the expressions of Wnt/β-catenin and estrogen pathway genes in Immp2l homozygous mutant mice, RNA sequencing in mouse ovaries was performed at 28 days of age, and the results were confirmed with

RT-quantitative PCR. A heat map and volcano plot of the differentially expressed mRNAs were generated and are presented in Supplemental Fig. 2A and 2B (28), respectively. There were 729 genes downregulated and 412 upregulated. Functional analysis of these differentially expressed mRNAs by gene ontology analysis identified 3 categories of genes closely related to female reproduction. These categories were developmental process, reproduction, and antioxidant activity (Supplemental Fig. 2C) (28). We also performed KEGG pathway analysis, which revealed 2 enriched pathways: the Wnt/β-catenin signaling pathway and the steroid hormone biosynthesis pathway (Supplemental Fig. 2D) (28). Indeed, hierarchical clustering of the differentially expressed mRNAs showed a clear distinction between the wild-type and Immp2l$^{-/-}$ mice ovaries. The Wnt pathway genes, including FZD10, Wnt16, FZD6, Lama3B, PIK3R2, Ppard, Ctnnb1 (β-catenin), and MECOM, and steroid hormone biosynthesis genes such as Cyp19a1, Cyp11a1, Arr1c18, and Cyp11b1 were affected in Immp2l$^{-/-}$ mice ovaries. Consistently, the expressions of these genes were confirmed by quantitative PCR.

Melatonin reversed the ovarian follicle growth retardation and ovarian aging in the Immp2l mutant mice

Melatonin was injected into Immp2l$^{-/-}$ mice at 14 days of age and continued daily until 28 days of age. Histology of the ovarian tissue revealed that ovarian follicle growth delay in the Immp2l$^{-/-}$ mice was reversed by melatonin treatment. As such, the number of antral follicles increased and secondary follicles decreased compared with non-melatonin-treated Immp2l$^{-/-}$ mice (Fig. 4). Further, melatonin significantly reduced the content of MDA and increased the level of GSH-Px in the serum of the Immp2l$^{-/-}$ mice (Fig. 5A, $P < 0.05$ vs. non-melatonin-treated Immp2l$^{-/-}$ mice). Moreover, there is a significant difference of MDA in melatonin-treated and non-melatonin-treated Immp2l$^{-/-}$ mice compared with control group (Fig. 5A, $P < 0.05$). Therefore, melatonin ameliorated the oxidative stress in the Immp2l$^{-/-}$ mice. Serum E_2 and AMH levels significantly decreased in the Immp2l$^{-/-}$ mice compared with the control group (Fig. 5B, $P < 0.05$), whereas they significantly increased in melatonin-treated Immp2l$^{-/-}$ mice compared with nontreated Immp2l$^{-/-}$ mice (Fig. 5B, $P < 0.05$). There was no significant difference of serum E_2 and AMH levels between melatonin-treated Immp2l$^{-/-}$ mice and control group.

Examination of Wnt/β-catenin and steroid hormone synthesis pathway-related genes and proteins in ovarian tissues of 28-day-old mice showed that homozygous mutation of Immp2l suppressed the gene expressions of Wnt16 and Cyp19a1 (Fig. 5C, $P < 0.05$ vs. Immp2l$^{+/+}$ mice), so did their proteins (Fig. 5D, $P < 0.05$ vs. Immp2l$^{+/+}$ mice). As expected, Immp2l$^{-/-}$ significantly increased the mRNA and protein levels of β-catenin

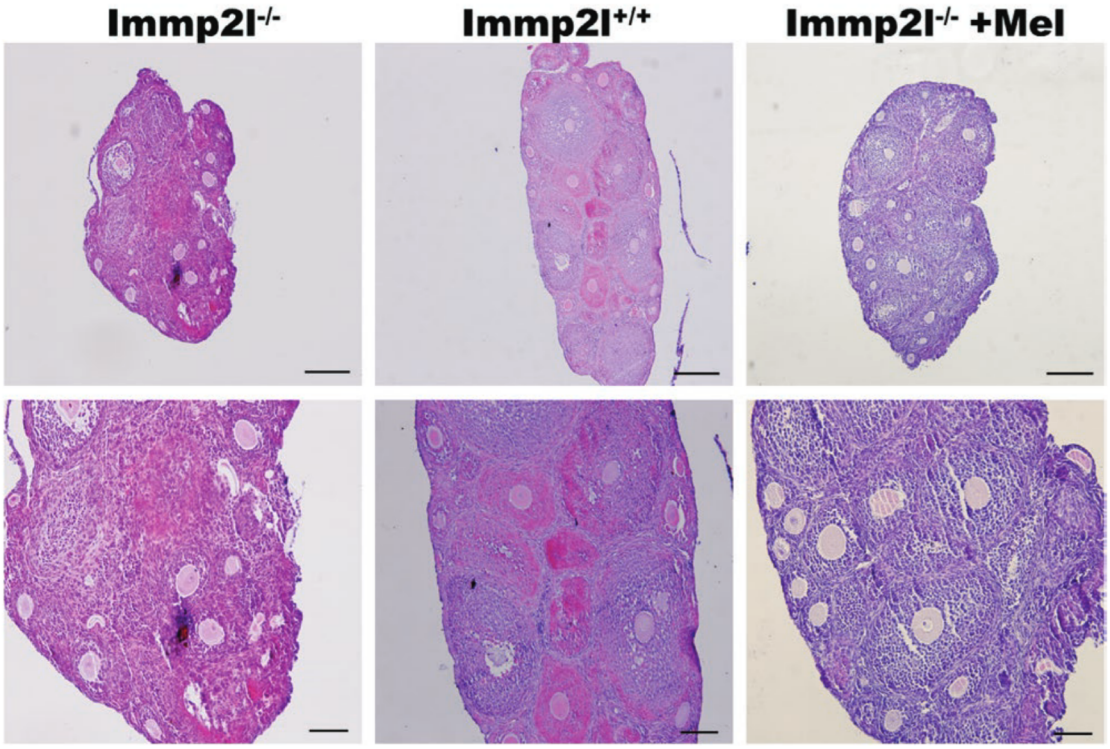

Figure 4. Ovarian morphology of 28-day-old Immp2l$^{-/-}$, Immp2$^{+/+}$, and Immp2l$^{-/+}$ melatonin-treated mice. Ovarian follicle growth was delayed in the Immp2l$^{-/-}$ mice and reversed by melatonin treatment. Upper figures' scale bar: 100 μm; lower figures' scale bar: 50 μm. Immp2l, inner mitochondrial membrane peptidase 2-like; Mel, melatonin.

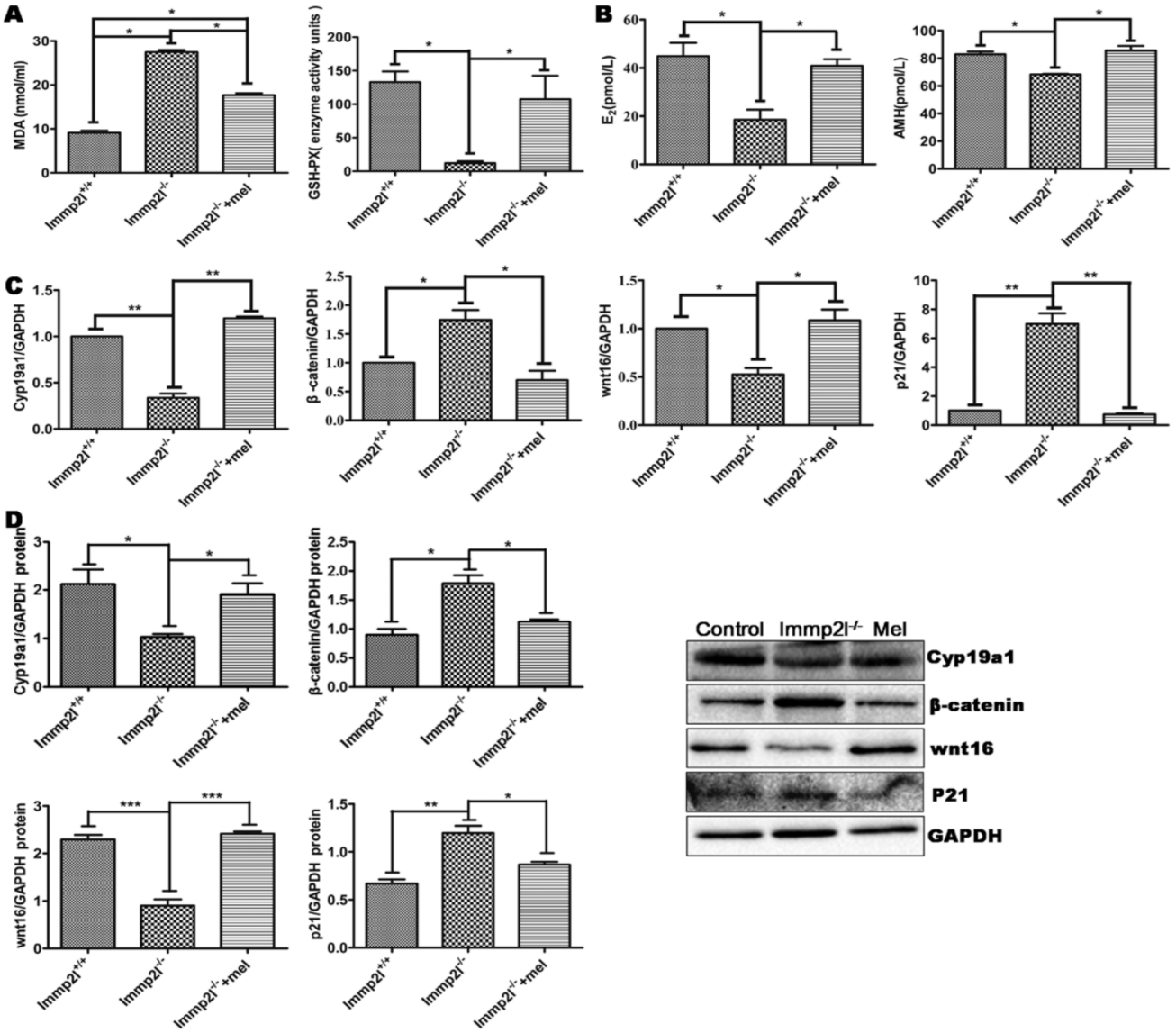

Figure 5. Oxidative stress markers, hormonal, and Wnt/β-catenin pathways in the ovaries of 28-day-old Immp2l$^{-/-}$ mice. (A) Serum ROS marker MDA increased and GSH-Px decreased in Immp2l$^{-/-}$ mice. (B) Serum E_2 and AMH were decreased in Immp2l$^{-/-}$ mice. (C) mRNA levels of cyp19a1 and wnt16 decreased, whereas β-catenin and P21 increased in Immp2l$^{-/-}$ mice. (D) Proteins of cyp19a1 and wnt16 decreased, and β-catenin and P21 increased in Immp2l$^{-/-}$ mice. Melatonin treatment reversed the alterations in Immp2l$^{-/-}$ mice. E_2, estrogen; GSH-Px, glutathione peroxidase; Immp2l, inner mitochondrial membrane peptidase 2-like; mel, melatonin; ROS, reactive oxygen species. *$P < 0.05$, **$P < 0.01$, ***$P < 0.001$.

and p21 (Fig. 5C and 5D, $P < 0.05$ vs. Immp2l$^{+/+}$ mice). Melatonin treatment almost entirely corrected the above alterations in the Immp2l$^{-/-}$ mice (Fig. 5C and 5D, $P < 0.05$ vs. Immp2l$^{-/-}$ mice). Immp2l$^{-/-}$ caused significantly decreased mRNA levels of FZD6, Lama3B, and MECOM and increased mRNA levels of FZD10, PIK3R2, and Ppard, all of which related to the Wnt/β-catenin pathway (Supplemental Fig. 3) (28). For the steroid hormone-related pathway, Immp2l$^{-/-}$ increased mRNA levels of Cyp11a1, Arr1c18, and Cyp11b1. Again, melatonin treatment successfully corrected all the aforementioned alterations in the Immp2l$^{-/-}$ mice (Supplemental Fig. 3) (28).

Additionally, examination of the ovaries of Immp2l$^{-/-}$ mice at 42, 49, 63, 77, 84, 98, and 154 days of age revealed that there was more corpus luteum in the ovaries and more ovarian follicles degenerated, and fewer ovarian follicles in Immp2l$^{-/-}$ mice at 154 days than those in wild-type mice (Supplement Fig. 4) (28). Long-term melatonin treatment for 5 months reversed these phenotypes observed in the Immp2l$^{-/-}$ mice and extended the ovarian lifespan (Fig. 6). Measurements of E_2 and AMH in the serum revealed that both E_2 and AMH levels significantly increased in the 100 mg/kg melatonin treatment group (Fig. 7A, $P < 0.05$), but no differences were found in the 200 mg/kg melatonin-treated Immp2l$^{-/-}$ animals compared with the Immp2l$^{-/-}$ mice. Additionally, 100 mg/kg of melatonin moderately, whereas 200 mg/kg significantly, increased serum MDA content (Fig. 7B, $P < 0.05$). Melatonin 100 mg/kg

increased the serum GSH-Px, whereas 200 mg/kg significantly decreased it, compared with Immp2l$^{-/-}$ mice (Fig. 7B, $P < 0.05$).

In addition, the western blot results suggested that the protein levels of Wnt16, β-catenin, and aging marker p21 significantly decreased, and those of cyp19a1 significantly increased, in a dose-dependent manner in the ovarian tissues of the Immp2l$^{-/-}$ mice treated with 100 and 200 mg/kg of melatonin (Fig. 7C) compared with the non-melatonin-treated Immp2l$^{-/-}$ mice (Fig. 7C, $P < 0.05$).

Melatonin administration in Immp2l knockdown granulosa cells

To further confirm the impact of Immp2l in the ROS-Wnt/β-catenin-estrogen (cyp19a1) pathway, we knocked down the *Immp2l* gene in granulosa cells and analyzed the ROS-Wnt/β-catenin-estrogen pathway. The MDA levels in the medium significantly increased in Immp2l knockdown granulosa cells, compared with the control groups (Fig. 8A, $P < 0.05$). Same as the results obtained in vivo, melatonin prevented the MDA increase that was observed in Immp2l knockdown granulosa cells (Fig. 8A, $P < 0.05$); the levels of GSH-Px and E_2 in the medium significantly decreased in Immp2l knockdown granulosa cells compared with the control groups (Fig. 8A, $P < 0.05$); these decreases were prevented by melatonin (Fig. 8A, $P < 0.05$). Consistent with the in vivo results, the expression of the cyp19a1 transcript and protein significantly decreased, whereas β-catenin increased in Immp2l knockdown granulosa cells compared with the control groups (Fig. 8B and 8C, $P < 0.05$), and the alternations were prevented by melatonin intervention (Fig. 8B and 8C, $P < 0.05$).

Additionally, P21 protein expression significantly increased in Immp2l knockdown granulosa cells compared with the control cells, whereas melatonin treatment blocked the increase (Fig. 8C, $P < 0.05$). In addition, the interaction of β-catenin and cyp19a1 in granulosa cells was detected with coimmunoprecipitation (co-IP), and the results suggested that β-catenin interacted with cyp19a1 in granulosa cells (Fig. 8D). Furthermore, β-catenin and cyp19a1 were colocalized in the cytoplasm and nucleus of granulosa cells. SiRNA Immp2l reduced the colocalization compared with control granulosa cells and melatonin slightly improved it (Fig. 9).

Melatonin protected mitochondrial function and delayed senescence in Immp2l knockdown granulosa cells

To explore the effect of melatonin on ROS and mitochondrial membrane potential, we incubated Immp2l knockdown granulosa cells with DHE and TMRM probes separately. The results showed that ROS levels remarkably increased in the Immp2l knockdown granulosa cells than in the control cells (Fig. 10A).

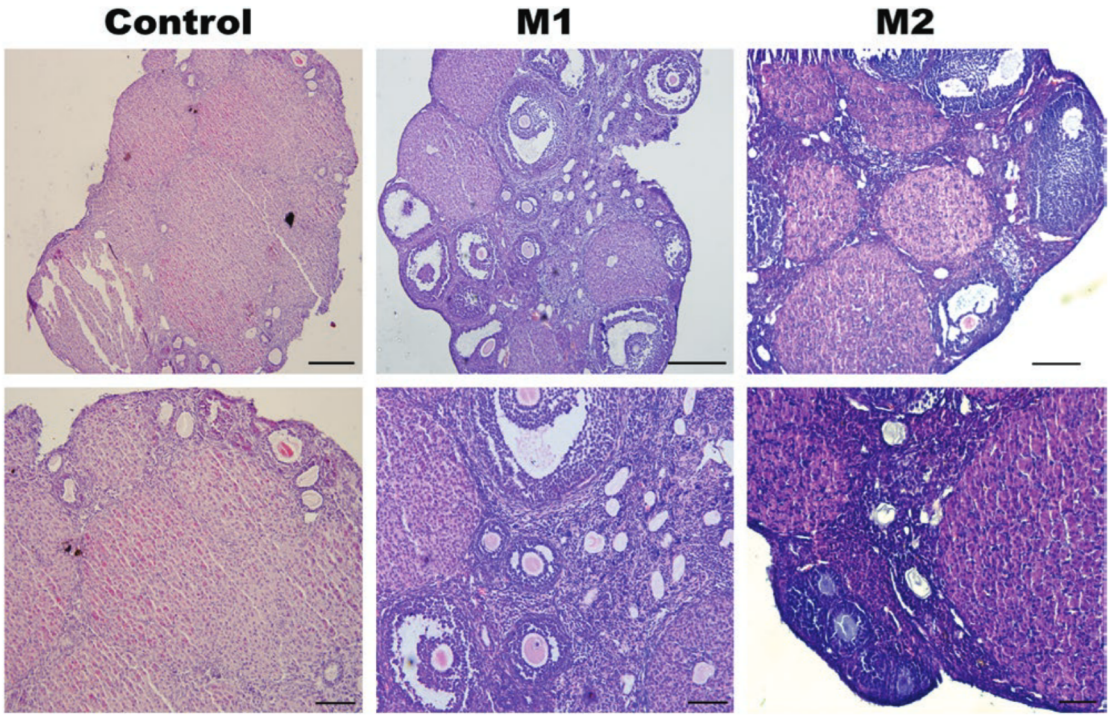

Figure 6. The effect of melatonin on ovarian morphology of 5-month-old Immp2l$^{-/-}$ mice. Melatonin treatment suppressed ovarian follicle degeneration in Immp2l$^{-/-}$ mice. Upper figures' scale bar: 100 μm; lower figures' scale bar: 50 μm. Con, nontreated control (Immp2l$^{-/-}$); Immp2l, inner mitochondrial membrane peptidase 2-like; M1, 100 mg/kg melatonin; M2, 200 mg/kg melatonin.

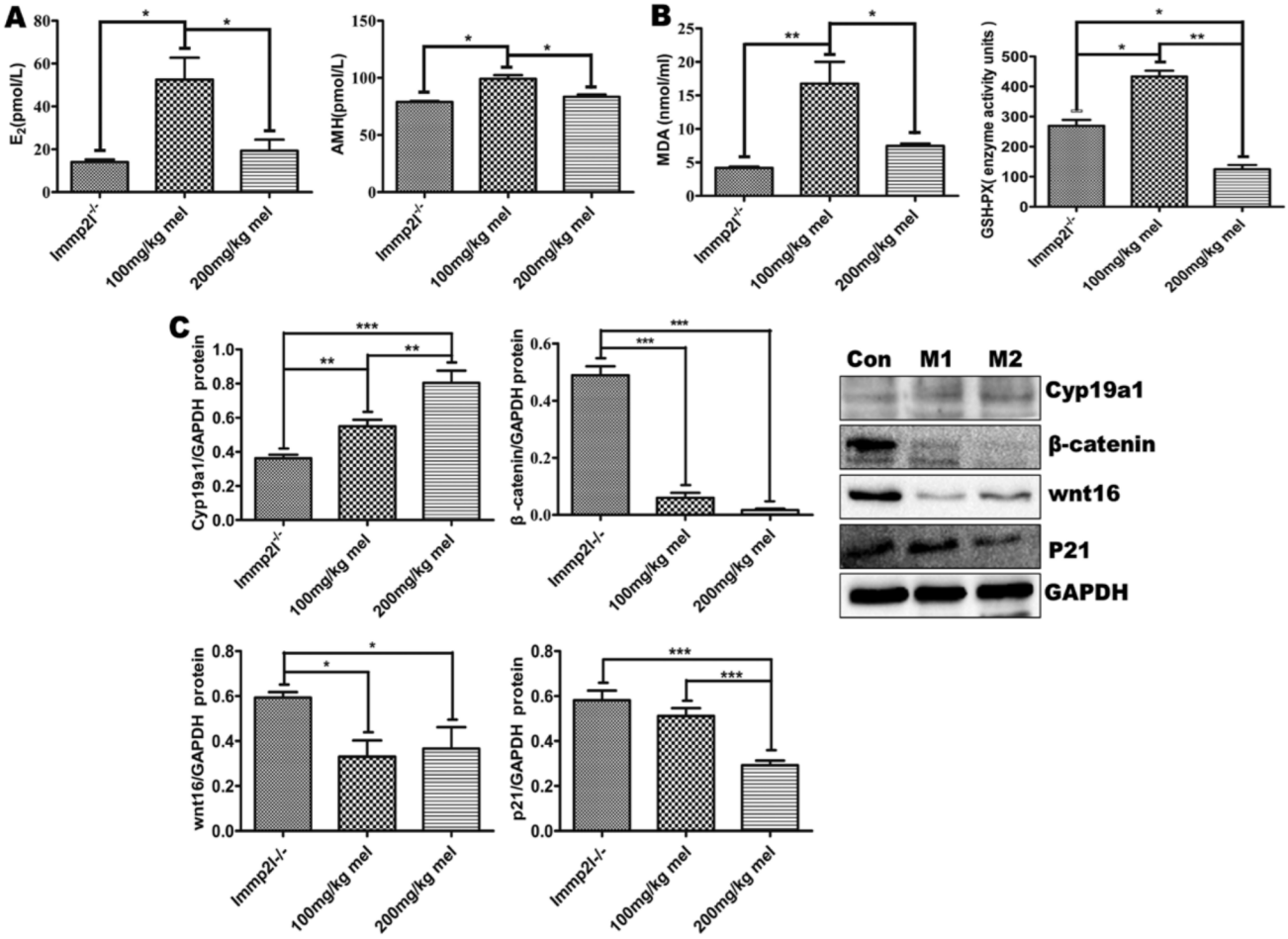

Figure 7. The effect of melatonin on oxidative stress markers, hormonal and Wnt pathways in 5-month-old Immp2l$^{-/-}$ mice. (A) Serum E_2 and AMH levels; (B) serum MDA and GSH-Px levels; (C) protein expression of cyp19a1, β-catenin, wnt16, and P21 in the ovaries. Con, nontreated control (Immp2l$^{-/-}$); Immp2l, inner mitochondrial membrane peptidase 2-like; M1, 100 mg/kg melatonin; M2, 200 mg/kg melatonin. *$P < 0.05$, **$P < 0.01$, ***$P < 0.001$.

Melatonin treatment prevented the ROS increase in the Immp2l knockdown granulosa cells (Fig. 10A). In contrast, TMRM staining revealed a decreased signal in the Immp2l knockdown granulosa cells compared with control cells, suggesting mitochondrial membrane potential depolarization. Melatonin treatment prevented the membrane depolarization in Immp2l knockdown granulosa cells (Fig. 10B). Compared with the control group, ATP levels significantly increased in the Immp2l and melatonin-treated Immp2l knockdown granulosa cells (Fig. 10C, $P < 0.05$). Additionally, melatonin reduced ATP levels in Immp2l knockdown granulosa cells, but there was no significant difference compared with Immp2l knockdown granulosa cells without melatonin treatment.

Immunocytochemistry using cell senescence marker β-Gal and γH2AX revealed that both β-Gal and γH2AX staining intensities were remarkably increased in the Immp2l knockdown granulosa cells compared with the control group, and the increases were ameliorated by melatonin in Immp2l knockdown granulosa cells (Fig. 10D and 10E). In addition, although the apoptotic granulosa cells increased in Immp2l knockdown groups as detected by Annexin-V/PI, there were no significant differences among the experimental groups (Fig. 11A) and the cell cycle was not altered (Fig. 11B).

Discussion

Mitochondrial dysfunction triggers ovarian dysfunction, infertility, and ovarian aging (5, 6). Although the role of *Immp2l*, a mitochondrial inner membrane gene, in several biological processes has been reported, the accurate role and mechanism of Immp2l in ovarian follicle development was not yet fully understood. In this study, we explored the role of Immp2l in ovarian follicle development and growth. Our results revealed that female Immp2l$^{-/-}$ mice were infertile, which is in agreement with the results of a previous study (12). In addition, we observed that the weights of ovary and body in female Immp2l homozygote mutant mice declined with

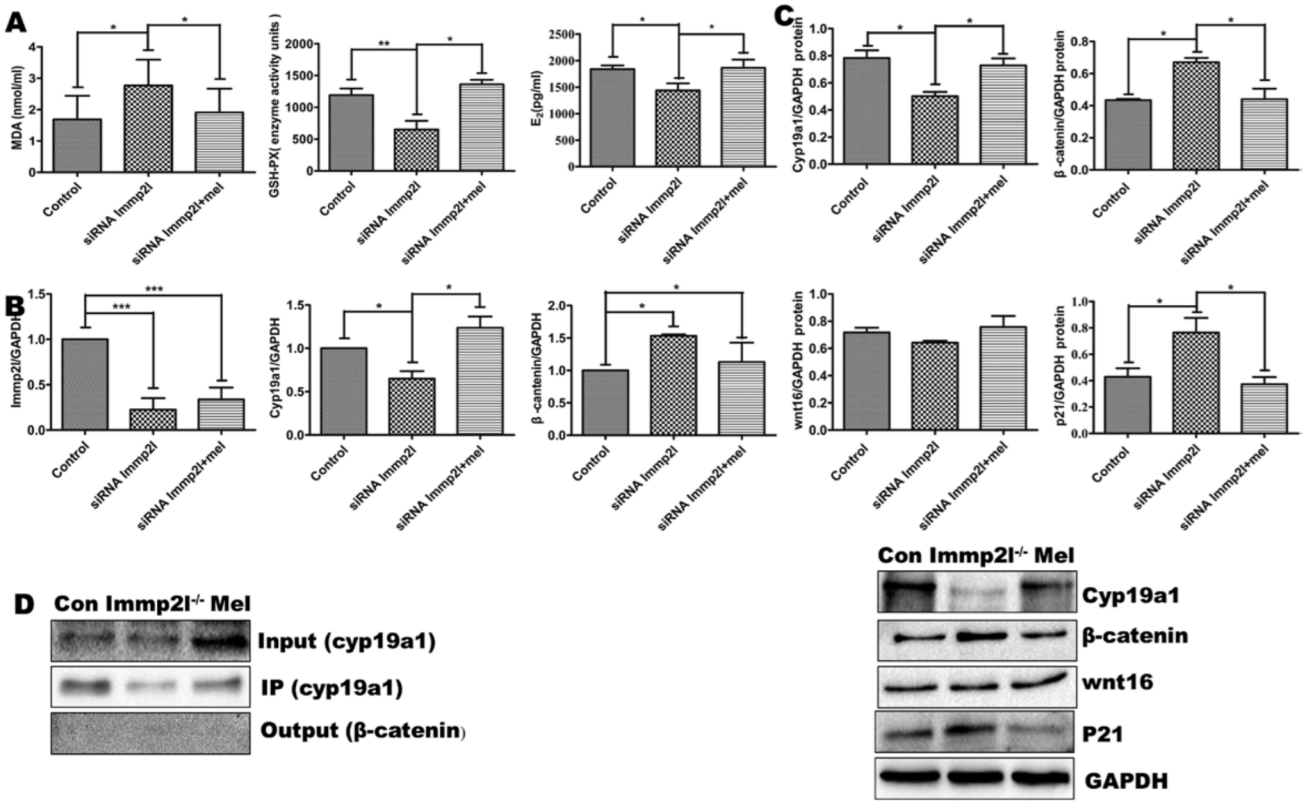

Figure 8. The effect of melatonin on oxidative stress markers, hormonal, and Wnt pathways in Immp2l knockdown granulosa cells. (A) MDA, GSH-Px, and E_2 levels in cell culture medium; (B) gene expression of Immp2l, cyp19a1, and β-catenin; (C) protein contents of cyp19a1,wnt16, β-catenin, and P21 in granulosa cells; (D) co-IP of β-catenin and cyp19a1 in granulose cells. co-IP, coimmunoprecipitation; con, control (scramble small interfering RNA); Immp2l, inner mitochondrial membrane peptidase 2-like; mel, melatonin. $*P < 0.05$, $**P < 0.01$, $***P < 0.001$.

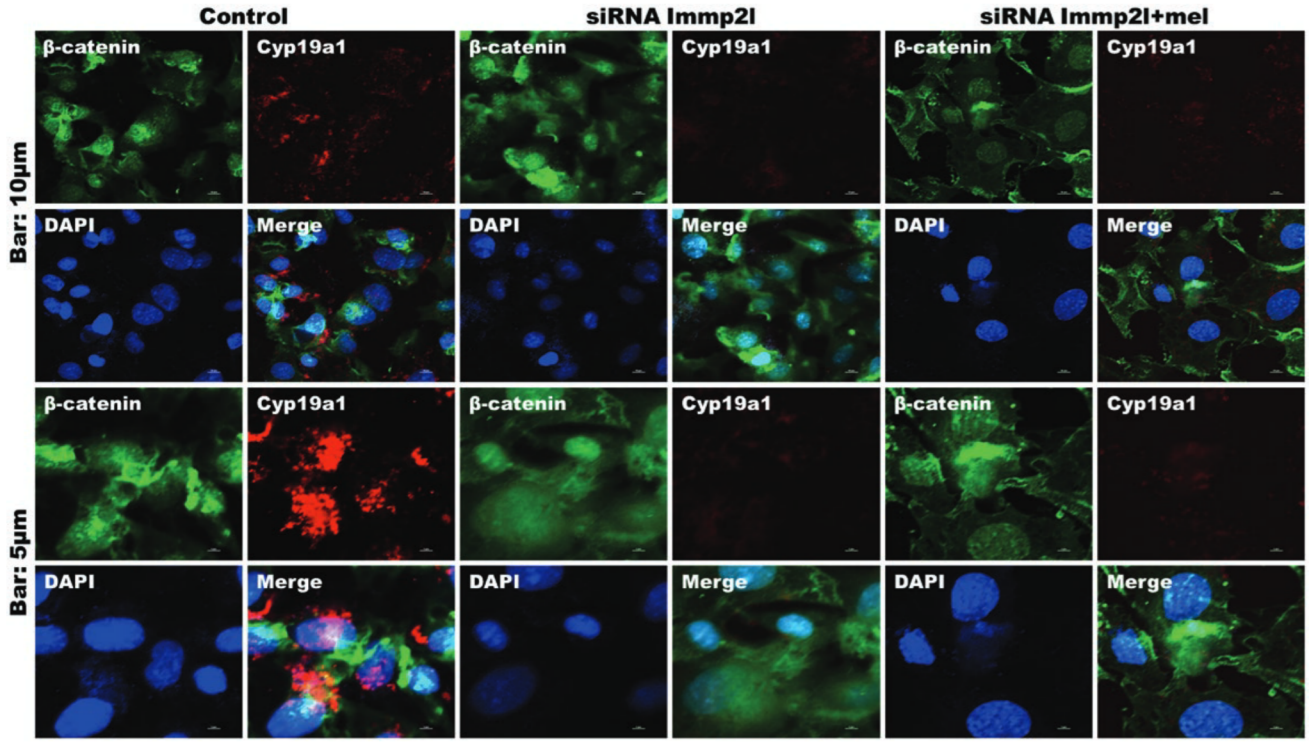

Figure 9. The colocalization of β-catenin (green color) and cyp19a1 (red color) in control granulosa cells, siRNA Immp2l granulosa cells, and siRNA Immp2l granulosa cells treated with melatonin. Green color, β-catenin; red color, cyp19a1; blue color, DAPI. Immp2l, inner mitochondrial membrane peptidase 2-like; siRNA, small interfering RNA.

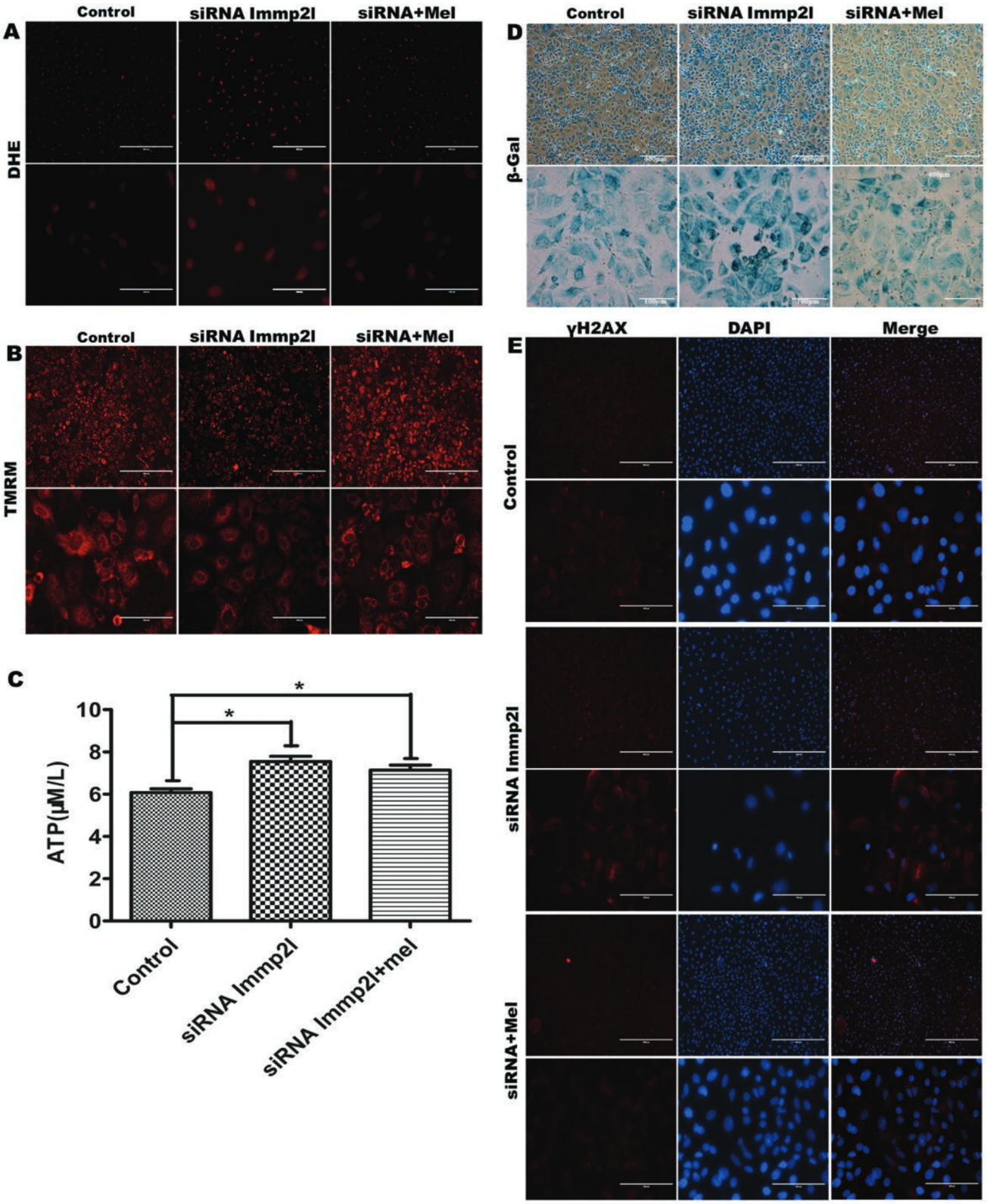

Figure 10. The detection of mitochondrial function and cell aging markers in control granulosa cells, siRNA Immp2l granulosa cells and SiRNA Immp2l granulose cells treated with melatonin. (A) ROS detected by DHE; (B) mitochondrial membrane potential detected by TMRE; (C) mitochondrial ATP production; (D) β-Gal staining; (E) γH2AX staining (red color) with nuclear labeling of DAPI (blue color). Immp2l, inner mitochondrial membrane peptidase 2-like; Mel, melatonin; ROS, reactive oxygen species; siRNA, small interfering RNA. $^{*}P < 0.05$, $^{**}P < 0.01$, $^{***}P < 0.001$.

age compared with the wild-type controls, which may be due to declining food intake through affecting nitric oxide signaling pathway (13).

To examine the underlying reasons by which female Immp2l homozygote mutant mice are infertile, we conducted histological assessments of the ovaries.

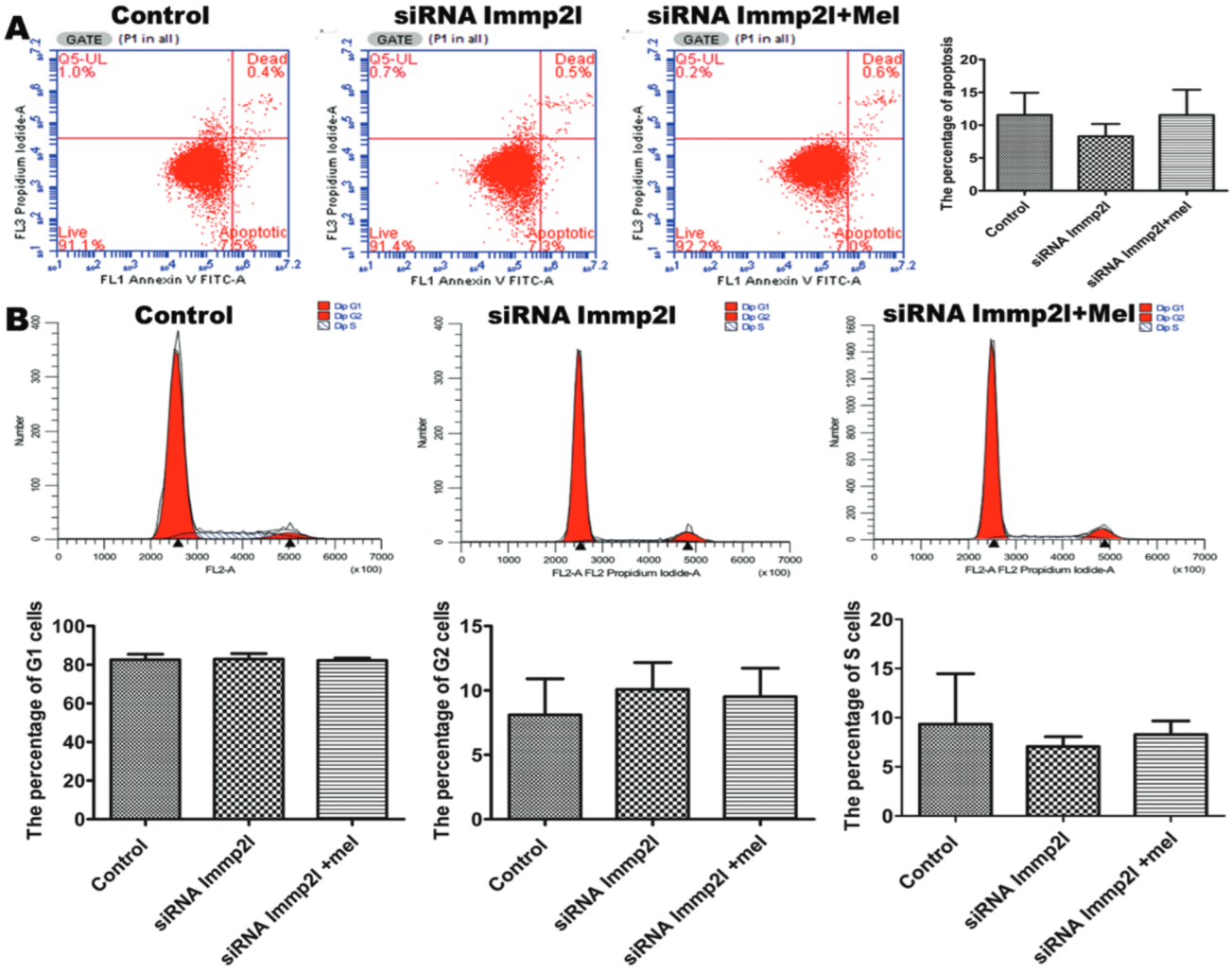

Figure 11. Detection of the cell cycle and apoptosis in control granulosa cells, siRNA Immp2l granulosa cells, and siRNA Immp2l granulosa cells treated with melatonin. (A) Detection of the apoptosis by Connexin V/PI using flow cytometer; (B) detection of the cell cycle. Immp2l, inner mitochondrial membrane peptidase 2-like; Mel, melatonin; siRNA, small interfering RNA. $*P < 0.05$, $**P < 0.01$, $***P < 0.001$.

The results showed that the ovarian follicle growth and development were delayed. In several female Immp2l$^{-/-}$ mice, only 1 or a few mature follicles were observed. Additionally, there were fewer ovulated oocytes in Immp2l homozygote mutant mice than in the wild-type animals, which may be ascribed to mitochondrial dysfunction in the mutant mice (12). Therefore, the infertility of Immp2l$^{-/-}$ mice is attributed to delayed ovarian follicle growth and development combined with oocyte dysfunction and ovarian aging.

Wnt/β-catenin and the steroid hormone play vital roles in regulating ovarian follicle development and growth (45). Our RNA-sequencing results revealed that Wnt/β-catenin and the steroid hormone pathway were activated in the ovary of Immp2l$^{-/-}$ mice. In particular, the canonical Wnt/β-catenin pathway marker β-catenin increased and the steroid hormone-related gene *cyp19a1* and serum estrogen decreased, accompanied with decreased ovarian reserve marker AMH (46, 47) in Immp2l$^{-/-}$ mice. Indeed, the Wnt pathway is involved in the development of ovarian follicles (21) and regulation of Cyp19a1, which encodes cytochrome P450 aromatase that converts androgens to 17β estradiol (E_2) (48).

Mitochondria are the primary resource of ROS, and physiological levels of ROS are essential for ovarian functions. However, excessive ROS may overpower the body's natural antioxidant defense system, accompanied by increased OS damage (7). Increased ROS were detected in Immp2l mutant mice serum, suggesting that OS damage was the main cause of delayed ovarian follicle growth and development. Additionally, OS damage initiated Wnt/β-catenin pathway involves in aging (49), reduces P450 aromatase expression, increases intracellular ROS generation, and alters Wnt signaling. Characterizing the granulosa cells of women with endometriosis (50) may emphasize that the ROS-Wnt/β-catenin-estrogen (cyp19a1) axis plays an important

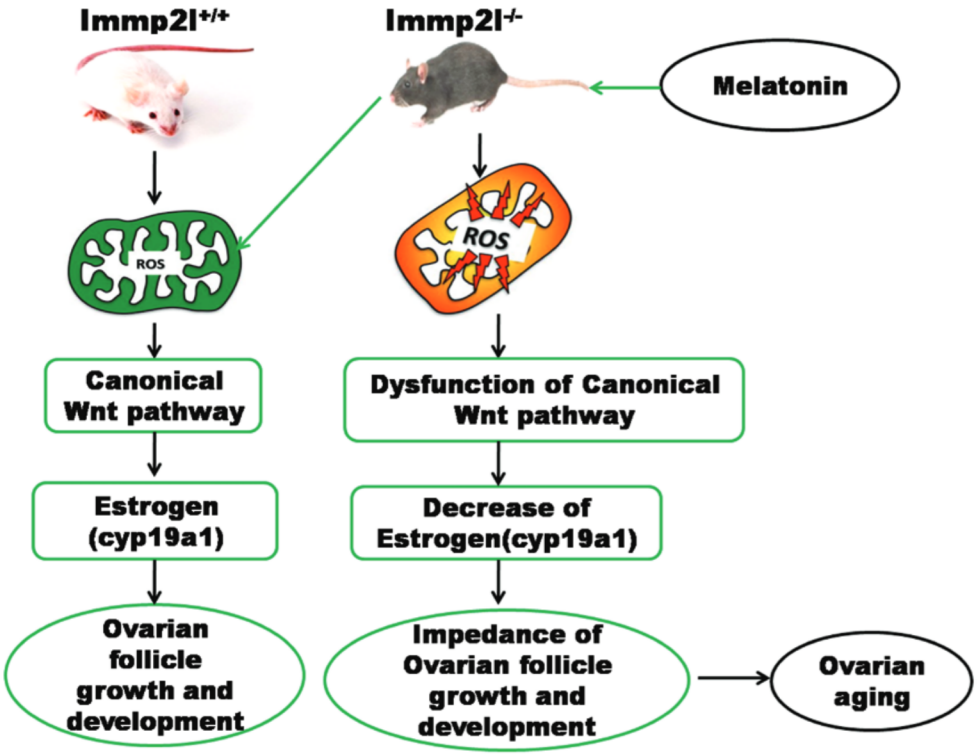

Figure 12. Schematic diagram showing mechanism of Immp2l gene deletion in ovarian aging. In wild-type animals, a normal amount of ROS maintains the balanced states of Wnt pathway and estrogen signaling for ovarian follicle growth and development. Deletion of Immp2l causes increased ROS production, which subsequently dysregulates the Wnt and estrogen signaling pathway and finally results in impedance of ovarian follicle growth and development and accelerates ovarian aging. Immp2l, inner mitochondrial membrane peptidase 2-like; ROS, reactive oxygen species.

role in maintaining ovarian follicle growth and development. These results might suggest that ovarian aging was caused by dysregulation of the ROS-Wnt/β-catenin-estrogen (cyp19a1) axis in Immp2l mutant mice.

As a vital antioxidant, the importance of melatonin in delaying ovarian aging was emphasized in our previous study (1). The aging phenotype of Immp2l mutant mice was reversed by the administration of melatonin, and the ovarian follicle growth and development delay were reversed. Consistently, the serum OS damage and decreased estrogen levels were improved, and the Wnt/β-catenin and estrogen pathways were also reversed. The activation of β-catenin regulates the mitochondrial function and protects against protein misfolding disorders (51). In this study, melatonin increased β-catenin expression and reduced the ROS in blastocysts (52). Indeed, the elevation of ROS and impaired Wnt/β-catenin signaling emphasized the role of ROS-Wnt.

β-catenin axis in the biological process (44), and ROS-Wnt/β-catenin was regulated by melatonin in the Immp2l mutant mice. Additionally, our results revealed that the treatment with melatonin improved estrogen and AMH levels, and increased the cyp19a1 expression in the Immp2l$^{-/-}$ mice. Consistent with the results in vivo, in vitro results from granulosa cells further confirmed that the ROS-Wnt/β-catenin-estrogen pathway was dysregulated in Immp2l knockdown granulosa cells. Indeed, several previous studies have revealed that overexpression of exogenous FZD3 in the human granulosa cell COV434 impaired long-term FSH incubation-induced cyp19a1 transactivation and the recruitment of β-catenin to Cyp19a1 promotor, and reduced the FSH-stimulated estrogen production (53). β-catenin participates in the follicle-stimulated hormone-mediated regulation of E_2 production in rat primary granulosa cells (54). The reduction of β-catenin significantly compromised the FSH stimulation of cyp19a1 mRNA and subsequent production of estradiol in primary granulosa cells (45). β-catenin, as an essential transcriptional regulator of cyp19a1, is present in transcription complexes assembled on the endogenous gonad-specific cyp19a1 promoter. Therefore, the expression of cyp19a1 and production of E_2 were controlled by β-catenin in granulosa cells. Our results from co-IP and colocalization of β-catenin and cyp19a1 protein in granulosa cells supported that β-catenin and cyp19a1 interacted in Immp2l knockdown granulosa cells.

A sharp increase in estrogen level triggers LH pulses, which is essential for ovulation. Therefore, a low amount of, or singular, oocyte ovulation in Immp2l$^{-/-}$ mice is probably from decreased cyp19a1 and serum estrogen levels. The increased oocyte ovulation in Immp2l$^{-/-}$ mice treated

with melatonin is likely associated with the increases of cyp19a1 and E_2 levels. Previous study has shown that melatonin upregulates cyp19a1 in granulosa cells (55). P21 has been reported as a marker of ovarian aging (56). In the present study, we observed an increased expression of P21 in Immp2l$^{-/-}$ mice, suggesting that accelerated ovarian aging is associated with Immp2l deficiency. Melatonin prolonged or even completely blocked ovarian aging in Immp2l$^{-/-}$ mice by suppressing the levels of P21. Consistently, the expression of other ovarian aging related markers, β-Gal (57) and γH2AX (58), was also detected by immunohistochemistry, the fluorescence intensities of β-Gal and γH2AX were remarkably increased in Immp2l knockdown granulosa cells, and was reversed by melatonin treatment. These results further support that Immp2l mutation accelerates and melatonin prolongs the ovarian aging. Our results showed that neither apoptosis nor the cell cycle were altered when Immp2l was knockdown in granulosa cells, consistent with the report showing that switching off Immp2l signaling drives cell senescence and the blockage of cell death (59).

Ovarian aging seriously affects the dynamic nature of mitochondrial biogenesis in the surrounding granulosa cells, which may provide interesting alternative biomarkers of oocyte quality (5) by producing excessive ROS in mitochondria and reducing mitochondrial membrane potential in Immp2l knockdown granulosa cells. Therefore, mitochondrial dysfunction of granulosa cell plays a critical role in ovarian aging (60). A previous study reported that the mitochondrial membrane potential and ATP levels were reduced in the aging granulosa cells (61). Melatonin has been shown to improve age-induced fertility decline and to attenuate ovarian mitochondrial oxidative stress (62). Additionally, the oocyte and granulosa cell interact with each other, and granulosa cells crucially regulate the ability of the oocyte to progress through the meiotic process and acquire full developmental potential (63, 64). The aging granulosa cells cause oocyte dysfunction. In present study, Immp2l deficiency caused the cease of ovarian follicle development could be a result of granulosa cell aging in the Immp2l mutation mice. Interestingly, our results demonstrated increased levels of ATP in Immp2l knockdown granulosa cells, which is consistent with the results from the cells of Immp2l mutant mice (12). This increase in ATP may be in response to increased inflammation and ROS because ATP is primarily a proinflammatory molecule (65, 66). Indeed, we observed increases of several inflammation factors in Immp2l mutant mice (data not shown). Taken together, the Immp2l mutation causes ovarian aging through activating the ROS-Wnt/β-catenin-estrogen (cyp19a1) pathway and melatonin delays ovarian aging in Immp2l mutant animals by suppressing the pathway (Fig. 12).

Acknowledgments

Financial Support: This work was supported by National Natural Science Foundation of China (81860262, 81760240, 81660690), National Natural Science Foundation of Ningxia (2020AAC02020), and Funds of Ningxia Medical University (XY201808), Key Research and Development Program of Ningxia (Grant 2019BFG2007), Ningxia Innovation Team of the Foundation and Clinical Researches of Diabetes and Its Complications (NXKJT2019010).

Author Contributions: Y.Y. designed the concept of the present study and supervised the project. Q.H., L.G., and Q.L. acquired, analyzed, and interpreted the data. Y.M. C.L., and X.P. supplied the methodology. Y.Y. and P.A.L. wrote and revised the manuscript.

Additional Information

Correspondence: Yanzhou Yang, Key Laboratory of Fertility Preservation and Maintenance, Ministry of Education, Key Laboratory of Reproduction and Genetics in Ningxia, Ningxia Medical University. E-mail: alnord820119@163.com. Orcid:Yanzhou Yang: https://orcid.org/0000-0002-1220-5164; or P. Andy Li, Department of Pharmaceutical Sciences, North Carolina Central University, Durham, NC 27707. E-mail: pli@neccu.edu.

Disclosure Summary: The authors declared that they have no conflicts of interest.

Data Availability: The datasets generated during and/or analyzed during the current study are not publicly available but are available from the corresponding author on reasonable request.

References

1. Yang Y, Cheung HH, Zhang C, Wu J, Chan WY. Melatonin as potential targets for delaying ovarian aging. *Curr Drug Targets*. 2019;**20**(1):16-28.
2. Broekmans FJ, Soules MR, Fauser BC. Ovarian aging: mechanisms and clinical consequences. *Endocr Rev*. 2009;**30**(5):465-493.
3. Li Q, Geng X, Zheng W, Tang J, Xu B, Shi Q. Current understanding of ovarian aging. *Sci China Life Sci*. 2012;**55**(8):659-669.
4. Hajjar C, Sampuda KM, Boyd L. Dual roles for ubiquitination in the processing of sperm organelles after fertilization. *BMC Dev Biol*. 2014;**14**:6.
5. May-Panloup P, Boucret L, Chao de la Barca JM, et al. Ovarian ageing: the role of mitochondria in oocytes and follicles. *Hum Reprod Update*. 2016;**22**(6):725-743.
6. Wang T, Zhang M, Jiang Z, Seli E. Mitochondrial dysfunction and ovarian aging. *Am J Reprod Immunol*. 2017;**77**:12651.
7. Wang XN, Zhang CJ, Diao HL, Zhang Y. Protective effects of curcumin against sodium arsenite-induced ovarian oxidative injury in a mouse model. *Chin Med J (Engl)*. 2017;**130**(9):1026-1032.
8. Pertynska-Marczewska M, Diamanti-Kandarakis E. Aging ovary and the role for advanced glycation end products. *Menopause*. 2017;**24**(3):345-351.
9. Liu C, Li X, Lu B. The Immp2l mutation causes age-dependent degeneration of cerebellar granule neurons prevented by antioxidant treatment. *Aging Cell*. 2016;**15**(1):167-176.
10. Ma Y, Mehta SL, Lu B, Li PA. Deficiency in inner mitochondrial membrane peptidase 2-like (Immp21) gene increases ischemic brain damage and impairs mitochondrial function. *Neuroboil Dis*. 2011;**44**:270-276.

11. George SK, Jiao Y, Bishop CE, Lu B. Oxidative stress is involved in age-dependent spermatogenic damage of Immp2l mutant mice. *Free Radic Biol Med*. 2012;**52**(11-12):2223-2233.
12. Lu B, Poirier C, Gaspar T, et al. A mutation in the inner mitochondrial membrane peptidase 2-like gene (Immp2l) affects mitochondrial function and impairs fertility in mice. *Biol Reprod*. 2008;**78**(4):601-610.
13. Han C, Zhao Q, Lu B. The role of nitric oxide signaling in food intake; insights from the inner mitochondrial membrane peptidase 2 mutant mice. *Redox Biol*. 2013;**1**:498-507.
14. Soler R, Füllhase C, Lu B, Bishop CE, Andersson KE. Bladder dysfunction in a new mutant mouse model with increased superoxide–lack of nitric oxide? *J Urol*. 2010;**183**(2): 780-785.
15. George SK, Jiao Y, Bishop CE, Lu B. Mitochondrial peptidase IMMP2L mutation causes early onset of age-associated disorders and impairs adult stem cell self-renewal. *Aging Cell*. 2011;**10**(4):584-594.
16. Willert K, Jones KA. Wnt signaling: is the party in the nucleus? *Genes Dev*. 2006;**20**(11):1394-1404.
17. Komiya Y, Habas R. Wnt signal transduction pathways. *Organogenesis*. 2008;**4**(2):68-75.
18. Angers S, Moon RT. Proximal events in Wnt signal transduction. *Nat Rev Mol Cell Biol*. 2009;**10**(7):468-477.
19. Castañon BI, Stapp AD, Gifford CA, Spicer LJ, Hallford DM, Hernandez Gifford JA. Follicle-stimulating hormone regulation of estradiol production: possible involvement of WNT2 and β-catenin in bovine granulosa cells. *J Anim Sci*. 2012;**90**(11):3789-3797.
20. Boyer A, Lapointe E, Zheng X, et al. WNT4 is required for normal ovarian follicle development and female fertility. *Faseb J*. 2010;**24**(8):3010-3025.
21. Hernandez Gifford JA. The role of WNT signaling in adult ovarian folliculogenesis. *Reproduction*. 2015;**150**(4):R137 -R148.
22. Crooke A, Huete-Toral F, Colligris B, Pintor J. The role and therapeutic potential of melatonin in age-related ocular diseases. *J Pineal Res*. 2017;**63**:12430.
23. Reiter RJ, Rosales-Corral S, Tan DX, Jou MJ, Galano A, Xu B. Melatonin as a mitochondria-targeted antioxidant: one of evolution's best ideas. *Cell Mol Life Sci*. 2017;**74**(21): 3863-3881.
24. Paradies G, Paradies V, Ruggiero FM, Petrosillo G. Protective role of melatonin in mitochondrial dysfunction and related disorders. *Arch Toxicol*. 2015;**89**(6):923-939.
25. Yang Y, Lin P, Chen F, et al. Luman recruiting factor regulates endoplasmic reticulum stress in mouse ovarian granulosa cell apoptosis. *Theriogenology*. 2013;**79**(4):633-9.e1.
26. Yang Y, Chen J, Wu H, et al. The increased expression of connexin and VEGF in mouse ovarian tissue vitrification by follicle stimulating hormone. *Biomed Res Int*. 2015;**2015**:397264.
27. Tilly JL. Ovarian follicle counts–not as simple as 1, 2, 3. *Reprod Biol Endocrinol*. 2003;**1**:11.
28. He Q, Gu L, Lin Q, et al. The Immp2l mutation causes ovarian aging through ROS-wnt/β-catenin-estrogen (cyp19a1) pathway: preventive effect of melatonin. 2020. Dryad, Dataset, ProMED-mail website. https://datadryad.org/stash/dataset/doi:10.5061/dryad.hmgqnk9db?.
29. RRID:AB_2233868. ProMED-mail website. https://antibodyregistry.org/search?q=15970-1-AP.
30. RRID:AB_2088670. ProMED-mail website. https://antibodyregistry.org/search?q=16554-1-AP.
31. RRID:AB_2857358. ProMED-mail website. https://antibodyregistry.org/search?q=66379-1-Ig.
32. RRID:AB_10862631. ProMED-mail website. https://antibodyregistry.org/search?q=ab109437.
33. RRID:AB_2734729. ProMED-mail website. https://antibodyregistry.org/search?q=ab188224.
34. RRID:AB_2857361. ProMED-mail website. https://antibodyregistry.org/search?q=AB_2857361.
35. RRID:AB_2857362. ProMED-mail website. https://antibodyregistry.org/search?q=AB_2857362.
36. RRID:AB_2857363. ProMED-mail website. https://antibodyregistry.org/search?q=AB_2857363.
37. Singhal NK, Srivastava G, Patel DK, Jain SK, Singh MP. Melatonin or silymarin reduces maneb- and paraquat-induced Parkinson's disease phenotype in the mouse. *J Pineal Res*. 2011;**50**(2):97-109.
38. Golabchi A, Wu B, Li X, et al. Melatonin improves quality and longevity of chronic neural recording. *Biomaterials*. 2018;**180**:225-239.
39. Tamura H, Kawamoto M, Sato S, et al. Long-term melatonin treatment delays ovarian aging. *J Pineal Res*. 2017;**62**:12381.
40. Shen M, Cao Y, Jiang Y, Wei Y, Liu H. Melatonin protects mouse granulosa cells against oxidative damage by inhibiting FOXO1-mediated autophagy: Implication of an antioxidation-independent mechanism. *Redox Biol*. 2018;**18**:138-157.
41. Del Rio D, Stewart AJ, Pellegrini N. A review of recent studies on malondialdehyde as toxic molecule and biological marker of oxidative stress. *Nutr Metab Cardiovasc Dis*. 2005;**15**(4):316-328.
42. de Oliveira Ulbrecht MO, Gonçalves DA, Zanoni LZG, do Nascimento VA. Association between selenium and malondialdehyde as an efficient biomarker of oxidative stress in infantile cardiac surgery. *Biol Trace Elem Res*. 2019;**187**(1):74-79.
43. Gugliandolo A, Gangemi C, Calabrò C, et al. Assessment of glutathione peroxidase-1 polymorphisms, oxidative stress and DNA damage in sensitivity-related illnesses. *Life Sci*. 2016;**145**:27-33.
44. Sun Y, Zheng Y, Wang C, Liu Y. Glutathione depletion induces ferroptosis, autophagy, and premature cell senescence in retinal pigment epithelial cells. *Cell Death Dis*. 2018;**9**(7):753.
45. Hernandez Gifford JA, Hunzicker-Dunn ME, Nilson JH. Conditional deletion of beta-catenin mediated by Amhr2cre in mice causes female infertility. *Biol Reprod*. 2009;**80**(6):1282-1292.
46. Wergedal JE, Kesavan C, Brommage R, Das S, Mohan S. Role of WNT16 in the regulation of periosteal bone formation in female mice. *Endocrinology*. 2015;**156**(3):1023-1032.
47. Amer SA, Shamy TTE, James C, Yosef AH, Mohamed AA. The impact of laparoscopic ovarian drilling on AMH and ovarian reserve: a meta-analysis. *Reproduction*. 2017;**154**(1):R13-R21.
48. Agarwal SK, Judd HL, Magoffin DA. A mechanism for the suppression of estrogen production in polycystic ovary syndrome. *J Clin Endocrinol Metab*. 1996;**81**(10):3686-3691.
49. Nie X, Liang L, Xi H, et al. 2, 3, 7, 8-Tetrachlorodibenzo-p-dioxin induces premature senescence of astrocytes via WNT/β-catenin signaling and ROS production. *J Appl Toxicol*. 2015;**35**(7):851-860.
50. Sanchez AM, Somigliana E, Vercellini P, Pagliardini L, Candiani M, Vigano P. Endometriosis as a detrimental condition for granulosa cell steroidogenesis and development: From molecular alterations to clinical impact. *J Steroid Biochem Mol Biol*. 2016;**155**(Pt A):35-46.
51. Jeong JK, Lee JH, Moon JH, Lee YJ, Park SY. Melatonin-mediated β-catenin activation protects neuron cells against prion protein-induced neurotoxicity. *J Pineal Res*. 2014;**57**(4):427-434.
52. Zhao XM, Min JT, Du WH, et al. Melatonin enhances the in vitro maturation and developmental potential of bovine oocytes denuded of the cumulus oophorus. *Zygote*. 2015;**23**(4):525-536.
53. Qiao GY, Dong BW, Zhu CJ, Yan CY, Chen BL. Deregulation of WNT2/FZD3/β-catenin pathway compromises the estrogen synthesis in cumulus cells from patients with polycystic ovary syndrome. *Biochem Biophys Res Commun*. 2017;**493**:847-854.
54. Stapp AD, Gómez BI, Gifford CA, Hallford DM, Hernandez Gifford JA. Canonical WNT signaling inhibits follicle stimulating hormone mediated steroidogenesis in

primary cultures of rat granulosa cells. *Plos One*. 2014;**9**(1): e86432.
55. Wang S, Liu W, Pang X, Dai S, Liu G. The mechanism of melatonin and its receptor MT2 involved in the development of bovine granulosa cells. *Int J Mol Sci*. 2018;**19**:E2028.
56. Papismadov N, Gal H, Krizhanovsky V. The anti-aging promise of p21. *Cell Cycle*. 2017;**16**(21):1997-1998.
57. Shimizu I, Minamino T. Cellular senescence in cardiac diseases. *J Cardiol*. 2019;**74**(4):313-319.
58. Zorin V, Grekhova A, Pustovalova M, et al. Spontaneous γH2AX foci in human dermal fibroblasts in relation to proliferation activity and aging. *Aging (Albany NY)*. 2019;**11**(13): 4536-4546.
59. Yuan L, Zhai L, Qian L, et al. Switching off IMMP2L signaling drives senescence via simultaneous metabolic alteration and blockage of cell death. *Cell Res*. 2018;**28**(6):625-643.
60. Tatone C, Amicarelli F. The aging ovary-the poor granulosa cells. *Fertil Steril*. 2013;**99**:12-17.
61. Liu Y, Han M, Li X, et al. Age-related changes in the mitochondria of human mural granulosa cells. *Hum Reprod*. 2017;**32**(12):2465-2473.
62. Song C, Peng W, Yin S, et al. Melatonin improves age-induced fertility decline and attenuates ovarian mitochondrial oxidative stress in mice. *Sci Rep*. 2016;**6**:35165.
63. Cecconi S, Ciccarelli C, Barberi M, Macchiarelli G, Canipari R. Granulosa cell-oocyte interactions. *Eur J Obstet Gynecol Reprod Biol*. 2004;**115**(Suppl 1):S19-S22.
64. Gilchrist RB, Ritter LJ, Armstrong DT. Oocyte-somatic cell interactions during follicle development in mammals. *Anim Reprod Sci*. 2004;**82-83**:431-446.
65. Vachharajani VT, Liu T, Wang X, Hoth JJ, Yoza BK, McCall CE. Sirtuins link inflammation and metabolism. *J Immunol Res*. 2016;**2016**:8167273.
66. Faas MM, Sáez T, de Vos P. Extracellular ATP and adenosine: the yin and yang in immune responses? *Mol Aspects Med*. 2017;**55**:9-19.